Research Square

Preprints are preliminary reports that have not undergone peer review.
They should not be considered conclusive, used to inform clinical practice,
or referenced by the media as validated information.

Province-Level Spatial Analysis of Climate Migration Risk in Türkiye Using an Indicator-Based Composite Index Approach

Mehmet Kadri Tekin

kadritekin@yyu.edu.tr

Van Yüzüncü Yıl Üniversitesi: Van Yuzuncu Yil Universitesi https://orcid.org/0000-0002-0667-6648

Murat Türkeş

Boğaziçi University: Bogazici Universitesi

Research Article

Keywords: climate migration, composite index, spatial risk, vulnerability, adaptive capacity, Türkiye

Posted Date: November 2nd, 2026

DOI: https://doi.org/10.21203/rs.3.rs-11103197/v1

License: This work is licensed under a Creative Commons Attribution 4.0 International License.
Read Full License

Province-Level Spatial Analysis of Climate Migration Risk in Türkiye Using an Indicator-Based Composite Index Approach

Abstract

This study maps relative climate migration risk across Türkiye's 81 provinces. Climate migration risk is conceptualized as the joint configuration of hazard, exposure, and vulnerability (sensitivity and adaptive capacity), rather than as a direct function of any single hazard. Twenty-five indicators from official statistics and international climate and land data were normalized to 0-1 within a theoretical hierarchy and combined into a fixed-weight linear Climate Migration Risk Index (CMRI). Robustness was assessed with equal and CRITIC weights, winsorization, geometric aggregation, leave-one-out analysis, and Monte Carlo simulation; the result was also compared diagnostically with the Turkish Statistical Institute's 2008–2025 internal migration series. Risk concentrates in southern and southeastern provinces, but similar scores arise from different combinations of hazards, agricultural exposure, social sensitivity, and capacity deficits. Alternative models preserve the main spatial pattern, whereas diagnostic migration comparisons show that structural risk and observed mobility should not be treated as equivalent constructs. The CMRI provides a transparent, reproducible, component-traceable link between national screening and place-based adaptation planning.

Keywords: climate migration; composite index; spatial risk; vulnerability; adaptive capacity; Türkiye

1. Introduction

Climate change is reshaping the conditions under which people sustain livelihoods where they live. Drought, extreme heat, floods, storms, and fires enter mobility decisions through production, water and food security, health, infrastructure, and household income. Yet the same hazard does not produce the same outcome everywhere. The size of the exposed population, the climate sensitivity of the economy, household resources, and the strength of public services influence whether a shock is met through in-situ adaptation, temporary mobility, permanent migration, or immobility (Black et al., 2011a; Cattaneo et al., 2019).

The central analytical difficulty is that physical pressure does not translate directly into a social decision. Environmental change commonly operates through intermediate mechanisms such as income, employment, food prices, health, security, and place attachment (Hunter et al., 2015; Piguet, 2010). Systematic evidence shows that effects vary by hazard, research design, and context and can be more visible where livelihoods depend on agriculture and institutional capacity is limited (Borderon et al., 2019; Hoffmann et al., 2020). Portraying high-risk populations as inevitable future "climate migrants" therefore obscures causal diversity and frames people as a passive security problem (Baldwin, 2013; Bettini, 2013; Boas et al., 2019).

Global projections provide a policy-relevant scale of warning. Under specified development and emissions scenarios, the World Bank projects that as many as 216 million people could move within their countries by 2050 (World Bank, 2021). This does not mean that everyone exposed to a hazard will migrate. Climate stress may amplify existing inequalities and livelihood difficulties, while the direction, timing, and form of movement depend on resources, migration networks, and destination conditions. The analytical need is therefore not to produce a single migration count, but to identify where structural conditions conducive to adverse mobility outcomes accumulate.

Türkiye combines heat and drought in the Mediterranean belt, extreme precipitation and flooding along the Black Sea, fire hazards in the Aegean and Mediterranean regions, and severe events in the interior and east. Drought probability, persistence, and socio-ecological vulnerability vary markedly, with several hotspots intensifying since 2000 (Çelik et al., 2026; Türkeş, 2017; Türkeş & Tatlı, 2009; Yurtseven & Türkeş, 2026). Heatwaves have increased in frequency, duration, and magnitude at many stations (Erlat et al., 2021). The recent expansion of semi-arid steppe and Mediterranean climates and contraction of cold climates already indicate warmer, drier conditions (Türkeş & Yurtseven, 2025). CMIP5 and CMIP6 similarly project stronger nationwide warming, declining precipitation especially in the south and west, and a more complex northern pattern (Bağçacı et al., 2021; Republic of Türkiye Ministry of Environment, Urbanisation and Climate Change, 2023, pp. 193-206; Yıldız et al., 2025).

Research on Türkiye has documented the biophysical and social dimensions of vulnerability to agricultural drought, desertification, and natural hazards (Serkendiz et al., 2023; Türkeş et al., 2020; Yükseler & Tenikler, 2025). International indicator-based spatial models similarly show that environmental and social conditions jointly shape vulnerability associated with rural migration (Schürmann et al., 2024). Although recent conceptual work on climate-related displacement and mobility (Türkeş et al., 2026) calls for hazard, vulnerability, adaptation, and the capacity to move to be considered together, this perspective has not yet been translated adequately into an uncertainty-tested measurement tool covering all Turkish provinces.

This study addresses that gap with an indicator-based composite index for all 81 provinces. It asks how hazard, exposure, sensitivity, and adaptive capacity vary; which component intersections produce high risk; and how stable provincial scores are under alternative methods and in relation to observed internal migration. The CMRI hierarchically combines 10 hazard, 3 exposure, 5 sensitivity, and 7 adaptive-capacity indicators.

The contribution extends beyond another provincial ranking. The study integrates multiple climate hazards with the social and institutional conditions that shape migration decisions in a common spatial framework. It identifies the mechanisms through which risk rises without detaching the final score from its underlying indicators and explicitly tests the effects of weighting, outliers, and aggregation. The CMRI is not an estimate of migration probability or causal effect; it is a diagnostic measure for

place-based investigation and adaptation prioritization. Section 2 develops the conceptual and analytical framework, Section 3 presents data and methods, Section 4 reports the results, and Sections 5 and 6 provide the discussion and conclusion.

2. Conceptual and analytical framework

2.1. Climate pressure, mobility, and adaptation

The relationship between climate and mobility operates through livelihoods, institutions, and decision-making rather than a simple hazard-response chain. Disrupted rainfall regimes, meteorological and agricultural drought, rising atmospheric evaporative demand, soil-moisture loss, and prolonged heatwaves can reduce yields, worsen working conditions, and compress household income. Migration is one possible outcome. Borrowing, crop switching, temporary labour, in-situ adaptation, and immobility occupy the same decision field. Reviews of quantitative research show that the relationship is sensitive to the definition of migration, time window, and spatial scale (Hoffmann et al., 2021; Schewel et al., 2024).

Empirical findings confirm this indirect relationship across contexts. The migration effects of very high temperatures and prolonged heatwaves can change direction with national income. In poor agricultural economies, resource loss may constrain movement rather than facilitate it (Beine & Parsons, 2015; Cattaneo & Peri, 2016). Evidence from Pakistan and South Africa, where temperature and precipitation anomalies affect rural mobility through agricultural livelihoods, shows that the hazard-migration link is embedded in production systems (Mastrorillo et al., 2016; Mueller et al., 2014). Sudden floods and fires may trigger short-term displacement, whereas drought and heat stress erode livelihoods over time. Even so, movement is not necessarily successful adaptation (Black et al., 2011b; Sakdapolrak et al., 2024).

The adaptive quality of migration depends less on movement itself than on its voluntariness, timing, and the rights and resources available afterward (McLeman & Smit, 2006). In the aspirations-capabilities framework, migration arises at the intersection of the aspiration to live elsewhere and the freedoms and resources needed to act on that aspiration (de Haas, 2021). Climate stress can increase the cost of staying while simultaneously reducing mobility capacity through income and asset losses. High structural risk therefore need not coincide with high recorded migration. Those able to move may leave selectively, while more vulnerable groups remain (Garip & Reed, 2025; Thomas et al., 2025).

Immobility is a critical test of this distinction. People may choose to stay because of place attachment, care responsibilities, or local livelihood knowledge, or may be unable to move because material and social resources are insufficient (Adams, 2016; Zickgraf, 2021). Cases in which place attachment and community capital jointly shape mobility decisions make this duality visible (Paul et al., 2020). In Türkiye, the overlapping climate and labour risks faced by seasonal agricultural workers, and the conversion of thermal-comfort seeking into local residential mobility in Antalya, likewise show that

no single form of migration is sufficient (Kavak et al., 2026; Ustaoğlu et al., 2026). The province-level CMRI compares the structural contexts in which individual decisions are made, not the decisions themselves.

2.2. Risk components and a spatial composite index

Risk is defined through hazard, exposure, and vulnerability. Hazard is the intensity, duration, or frequency of a potentially harmful climatic event; exposure is the presence of people and assets; sensitivity is predisposition to harm; and adaptive capacity comprises the economic, human, infrastructural, and institutional resources that reduce impacts (Intergovernmental Panel on Climate Change [IPCC], 2022, p. 5). Vulnerability is therefore contingent on the system, hazard, and scale, not a fixed property of place (Füssel, 2007).

This distinction accords with the foundations of social-vulnerability research. Demography, socioeconomic resources, housing, and access to services systematically differentiate the social consequences of hazards (Cutter et al., 2003), and the vulnerability of the same place can change over time (Cutter & Finch, 2008). The influence of indicators such as age, income, and housing is also context dependent, so selection must follow the harm mechanism being represented (Rufat et al., 2015). Sensitivity and capacity indicators were therefore chosen not to reproduce a general development ranking, but to represent channels through which climate stress may affect livelihoods and mobility options.

Composite indices combine information measured in different units on a common scale. Indicator selection, normalization, weighting, and aggregation can nevertheless alter rankings. Reliability depends on explicit justification of these decisions and on uncertainty analysis (Greco et al., 2019; Organisation for Economic Co-operation and Development [OECD] & European Commission, Joint Research Centre, 2008, pp. 13-14). Empirical work also shows that the indicator set, scale, and hierarchy can change vulnerability maps (Hinojos et al., 2026). The resulting map should therefore be read as a model built on transparent assumptions rather than a definitive reality (Preston et al., 2011; Tate, 2013).

Geographic information system-based multicriteria decision analysis combines environmental and social indicators in the same geographic unit, making the calculation chain spatially traceable (Malczewski, 2006; Mijani et al., 2022). Here, dry days represent hazard, agricultural land represents exposure, agricultural employment represents sensitivity, and irrigation infrastructure represents capacity. Because these measures describe different functions within the same production system, they remain in separate components. Presenting sub-indices alongside the final score both limits double counting and reveals the different risk pathways that can produce the same CMRI level.

2.3. Analytical model and expectations

The model has two levels. First, hazard (H), exposure (E), sensitivity (S), and adaptive capacity (AC) measure structural climate-mobility pressure. Second, the CMRI is compared with alternative scenarios and observed migration. Migration therefore does not become a self-explanatory index input. Migration variables are not CMRI inputs; they are used only for diagnostic comparison (Figure 1).

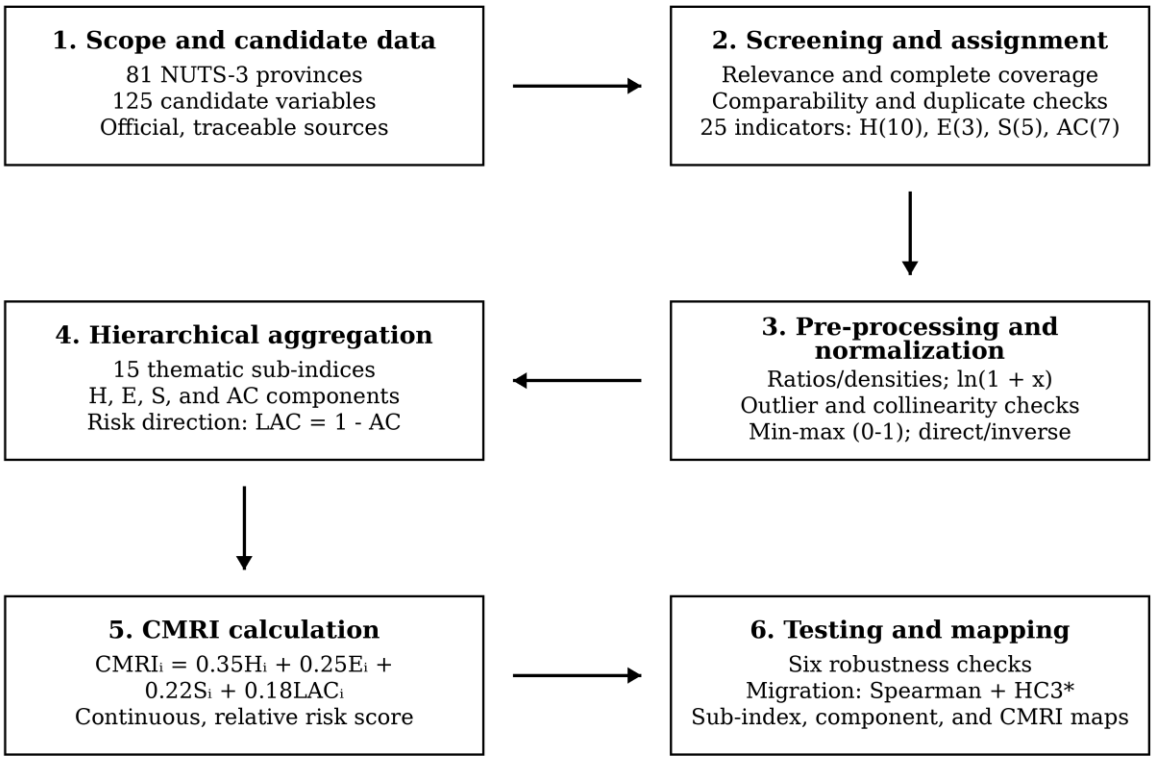


Figure 1. Workflow for data selection, index construction, robustness assessment, and diagnostic comparison

* Migration variables are not CMRI inputs; they are used only for diagnostic comparison.

The CMRI should rise as H, E, and S increase and AC declines. Similar scores may reflect different components, so the map requires the sub-indices. Because observed migration is multi-causal and selective, no perfect, linear, or uniformly signed relationship with migration rates is expected. Evaluation emphasizes component profiles, the high-score core retained across methods, and convergence with or divergence from recorded migration rather than exact ranks.

3. Data and methods

3.1. Research design and data selection

The analysis covers Türkiye's 81 NUTS-3 provinces. An initial set of 125 variables was screened for theoretical relevance, complete and consistently defined coverage, traceability, temporal comparability, reproducibility, and double counting. The final 25 cover climate, severe events recorded by the Turkish State Meteorological Service (MGM), population, land use, labour, households, health, irrigation, and local fiscal capacity. No missing, interpolated, or neighbouring-province-derived values enter the main model.

Indicator reduction reflected parsimony and conceptual separation. Duplicates, province-specific records, migration outcomes, and measures lacking reliable provincial counterparts were excluded. Drought, extreme heat, extreme precipitation-flood, storm, hail, frost, and fire pathways were retained. Each social indicator was assigned once, as exposure, predisposition to harm, or an impact-reducing resource.

Time windows match the process measured: 1991–2020 for climate normals, the 1991–2024 trend for drying, multiyear records for rare events, and the latest complete period for social and institutional indicators. This prioritizes process relevance and national comparability over formal simultaneity (Table 1).

Table 1. Data groups used in the main model

Indicator group	Indicators	Period	Source	Role in the model
Drought and extreme heat	CDD, SPEI-12 trend, HD35, WSDI	1991–2020; 1991–2024	Hersbach et al. (2020); World Bank (2026)	Duration, trend, and heat stress
Extreme precipitation and severe meteorological events	RX1day; flood, storm, hail, and frost densities	1991–2020; 2008–2022	Eurostat (2024); Meteoroloji Genel Müdürlüğü [MGM] (2023); World Bank (2026)	Intensity and observed event frequency
Wildfire	Burned-area density	2013–2021	Orman Genel Müdürlüğü [OGM] (2022)	Observed fire impact
Human and agricultural exposure	Population, population density, share of agricultural land	2025; CLC 2018	Copernicus Land Monitoring Service (2018); Türkiye İstatistik Kurumu [TurkStat] (2026)	Exposed population and production area
Social sensitivity	Age dependency, unemployment, registered agricultural employment, renting, large households	2021–2025	Sosyal Güvenlik Kurumu [SGK] (2025); Türkiye İstatistik Kurumu (2026)	Care, livelihood, labour, and household sensitivity
Adaptive capacity	GDP per capita, higher education, health care, irrigation, and local budget revenue per capita	2023–2024	Devlet Su İşleri Genel Müdürlüğü [DSİ] (2025); Hazine ve Maliye Bakanlığı (2026); T.C. Sağlık Bakanlığı (2024, pp. 253–254; 2025, pp. 133, 160, 162–163); Türkiye İstatistik Kurumu (2026)	Material, human, infrastructural, and fiscal resources

Note. CDD = maximum consecutive dry days; SPEI-12 = 12-month Standardized Precipitation Evapotranspiration Index; HD35 = number of days with a maximum temperature of at least 35 °C; WSDI = Warm Spell Duration Index; RX1day = annual maximum one-day precipitation; CLC = CORINE Land Cover; MGM = Turkish State Meteorological Service; TurkStat = Turkish Statistical Institute; SGK = Social Security Institution; DSİ = General Directorate of State Hydraulic Works.

Period differences reflect process time scales, not data incompatibility: long-term climate measures capture structural physical pressure, while the latest complete social data capture current response conditions.

3.2. Hierarchy, pre-processing, and normalization

Each indicator was assigned by mechanism to a subdimension and then H, E, S, or AC. This two-level hierarchy groups similar functions and prevents the 10-variable H component from dominating by count. Hazard, exposure, and sensitivity increase risk; income, education, health, irrigation, and local fiscal resources increase AC. Population per family-medicine unit measures service burden and was reverse-coded.

Raw counts were converted to comparable denominators. Flood, storm, hail, and frost were expressed as annual events per 10,000 km², and burned area as annual hectares per 10,000 km², using NUTS 2024 areas (European Commission, Eurostat, 2024). Physicians and beds were divided by population, irrigated area by agricultural area, and local budget revenue by population. Strongly right-skewed density, population, and economic variables with true zeros used ln(1 + x). Verified outliers remained in the main model and were tested through winsorization.

CDD, HD35, WSDI, and RX1day are area-weighted provincial means from ERA5 0.25° cells (Hersbach et al., 2020); SPEI-12 jointly represents precipitation and atmospheric evaporative demand (Vicente-Serrano et al., 2010). Min–max normalization rescaled variables to 0–1. Equation (1) gives direct (N^+) and inverse (N^-) directions.

$$N_{ij}^{+} = \frac{x_{ij} - \min_i(x_{ij})}{\max_i(x_{ij}) - \min_i(x_{ij})}, \qquad N_{ij}^{-} = \frac{\max_i(x_{ij}) - x_{ij}}{\max_i(x_{ij}) - \min_i(x_{ij})} \tag{1}$$

The SPEI-12 trend was inversely normalized because more negative values indicate stronger drying; other measures follow their theoretical direction. Values of 0 and 1 indicate relative, not absolute, safety or risk. Redundancy was checked using Spearman correlation and VIF thresholds of $|\rho| \geq 0.80$ and VIF ≥ 5.00. The maximum VIF was 4.675. CDD and HD35 were retained despite high correlation because they measure rain-free persistence and an absolute heat threshold, respectively, without exceeding the VIF limit.

Table 2. Model hierarchy and final weights

Main component	Subdimension (within-component weight)	Indicator (within-subdimension weight)	CMRI weight
Hazard (H)	Drought (0.30)	CDD (0.40); SPEI-12 trend (0.60)	0.35
	Extreme heat (0.20)	HD35 (0.50); WSDI (0.50)	

Main component	Subdimension (within-component weight)	Indicator (within-subdimension weight)	CMRI weight
	Extreme precipitation and flood (0.20)	RX1day (0.40); flood density (0.60)	
	Severe meteorological events (0.15)	Storm (0.40); hail (0.30); frost (0.30)	
	Wildfire (0.15)	Burned-area density (1.00)	
Exposure (E)	Human exposure (0.60)	Population (0.5833); population density (0.4167)	0.25
	Agricultural land exposure (0.40)	Share of agricultural land (1.00)	
Sensitivity (S)	Demographic sensitivity (0.15)	Age-dependency ratio (1.00)	0.22
	Livelihood and labour sensitivity (0.50)	Unemployment (0.40); registered agricultural employment (0.60)	
	Housing and household sensitivity (0.35)	Renter households (0.4286); households with 6+ members (0.5714)	
Adaptive capacity (AC)	Economic capacity (0.20)	GDP per capita (1.00)	0.18 × (1 − AC)
	Educational capacity (0.15)	Share of higher-education graduates (1.00)	
	Health-system capacity (0.25)	Physicians (0.40); beds (0.30); family-medicine workload (0.30)	
	Irrigation capacity (0.25)	Irrigated area/agricultural area (1.00)	
	Local fiscal capacity (0.15)	Local budget revenue per capita (1.00)	

Note. Values in parentheses are shares at the corresponding hierarchical level; weights sum to 1.00 at each level. AC is calculated in the positive capacity direction and converted within the CMRI to lack of adaptive capacity (LAC = 1 − AC). Panels k-o of Figure 2 and the lower-right panel of Figure 3 are shown in the LAC direction. This cartographic transformation does not change the component calculation.

The hierarchy separates final weights from indicator counts. H, with 10 indicators, and E, with three, are first scaled internally; no component therefore gains additional influence on the CMRI simply by containing more variables.

3.3. Weighting and CMRI calculation

The baseline coefficients were specified a priori as literature- and mechanism-informed normative weights, considering Türkiye's multi-hazard setting, indicator specificity, data quality, and conceptual relevance. H receives 0.35 because it directly represents climate pressure, E receives 0.25 for the spatial magnitude of exposure, S receives 0.22 for predisposition to harm, and the capacity deficit receives 0.18. Within each main component, subdimension and indicator weights were assigned to reflect their intended theoretical contribution to the represented mechanism and were normalized to sum to 1.00 at the corresponding hierarchical level. These are not universal coefficients prescribed by the IPCC. The influence of this normative specification was therefore tested under alternative weighting scenarios (OECD & European Commission, Joint Research Centre, 2008, pp. 83-85, 96-104). Table 2 reports the subdimension and indicator weights.

Each component is the weighted sum of normalized indicators within subdimensions and then of subdimensions. In Equation (2), N_{ij} is the normalized indicator, w_jd the indicator weight, wd_k the subdimension weight, and C_{ik} province i's H, E, S, or AC value. Weights sum to 1.00 at each level.

$$C_{ik} = \sum_{d=1}^{q_k} w_{dk} \left(\sum_{j=1}^{m_d} w_{jd} N_{ij} \right) \quad (2)$$

AC was calculated positively and converted for the final index and risk maps as LAC = 1 − AC; high values in H, E, S, and LAC therefore increase risk. Weighted linear combination preserves component contributions and prevents a sample minimum from reducing the total score to zero (Malczewski, 2000).

$$\mathrm{CMRI}_i = 0.35H_i + 0.25E_i + 0.22S_i + 0.18(1 - AC_i) \quad (3)$$

Equation (3) yields a continuous relative score: 0.60 is not a 60% migration probability. Linear aggregation permits limited compensation among components. Geometric aggregation, which more strongly restricts compensation of low by high values, tests whether this assumption drives the result.

3.4. Robustness, migration comparison, and cartographic presentation

Sensitivity to methodological choices was examined through six checks: hierarchical equal weighting, within-component CRITIC weighting, winsorization at the 2.5th and 97.5th percentiles, geometric aggregation, leave-one-out analysis in which each indicator was removed in turn, and Monte Carlo weight uncertainty with 5,000 draws. CRITIC combines variability with non-redundant information across indicators and was applied separately within each main component so that components containing more indicators would not gain an advantage (Diakoulaki et al., 1995). In the Monte Carlo analysis, 5,000 alternative weight sets were generated by perturbing the baseline weights within ±20% of their original values and renormalizing them to sum to 1.00 after each draw; a fixed random seed (20260826) was used to ensure reproducibility. Scenarios were compared using rank correlation, mean rank change, overlap in the top 20%, and province-specific 5th-95th percentile intervals (Saisana et al., 2005; Tate, 2012).

Migration variables are not index inputs. Verified counts of in-, out-, and net migration from the 2008–2025 provincial panel (Türkiye İstatistik Kurumu [TurkStat], 2026) were converted to rates. Because foreign nationals entered the series in 2018, mean 2018–2025 net migration is the primary longitudinal measure and 2008–2025 a coverage-break sensitivity check. The 2025 net and out-migration rates and the number of negative-net-migration years in 2018–2025 were also calculated.

Associations were first examined with Spearman rank correlation and then with linear models in which each migration indicator was the dependent variable and the CMRI the principal explanatory variable. The models controlled for a binary indicator identifying provinces affected by the 2023 earthquakes (1 = affected, 0 = otherwise) and the 2025 share of foreign nationals in the provincial population. These controls were included to account for a major non-climatic displacement shock and differences in population composition that may influence recorded internal migration independently of the CMRI. All p values are two-sided. Spearman coefficients use a Student's t approximation (df =

79), and linear-model coefficients use HC3 robust standard errors with a Student's t reference distribution (residual df = 77) (MacKinnon & White, 1985). The significance level was set a priori at $\alpha = 0.05$; $p \geq 0.05$ was not considered statistically significant. Continuous variables were standardized. This is neither a criterion-validity nor a causal test, but a diagnostic comparison of the extent to which structural risk and recorded mobility converge. Net migration is the balance of inflows and outflows, whereas the out-migration rate measures departure intensity; both are also shaped by education, employment, housing, life course, and migration networks.

H, E, S, LAC, and CMRI were joined to provincial boundaries. The 25 indicators form 15 thematic sub-indices. Figure 2 uses five equal classes over 0–1 in a common risk direction; Figure 3 uses seven equal classes within each component's observed range; Figure 4 uses 10 across the observed CMRI range. Classes aid visualization only; calculations use continuous values. The final matrix has 81 unique provinces and 25 complete indicators. Periods are not fully synchronous. The 0.25° grid misses microclimates, event records may contain reporting differences, and provincial means conceal internal inequality. Registered agricultural employment omits informal work, GDP per capita omits income distribution, and local budgets do not measure actual climate-adaptation spending.

4. Results

4.1. Spatial patterns of thematic sub-indices

The hazard sub-indices do not form a single national gradient. Drought and extreme heat overlap broadly in the south and southeast, whereas extreme precipitation-flood risk is prominent along the northern coast and in some western provinces, and wildfire risk is concentrated in the southwest and along the southern coast. More fragmented patterns of storms, hail, and frost in the interior interrupt this continuity. A source and calculation audit of panel (d) confirmed that Nevşehir's high value is unrelated to the 2025 agricultural frost; the sub-index uses only 2008–2022 event records. In its sub-index score of 0.934, the relative contributions of storms, hail, and frost are 35.7%, 32.1%, and 32.1%, respectively. The pattern therefore reflects the combined elevation of three indicators rather than one event. H consequently represents a portfolio of distinct, locally intersecting climate pressures rather than repeated versions of the same surface (Figure 2a-e).

Exposure follows two spatial logics: metropolitan provinces score highly through population size and density, while parts of Central Anatolia and Thrace do so through agricultural land. Similar E values therefore imply different priorities—housing and infrastructure continuity in metropolitan profiles, and production areas and rural livelihoods in agricultural profiles (Figure 2f-g).

Sensitivity also lacks one disadvantage surface. Demographic and housing–household burdens are more continuous in the east and southeast, while livelihood and labour sensitivity is fragmented across different agricultural and labour-market settings. S identifies places where care burdens, livelihood

dependence, and housing insecurity require joint inquiry, not which group will be harmed (Figure 2h-j).

Adaptive-capacity subdimensions are mapped as deficits, so high values denote scarcer resources and greater risk. Economic and educational deficits are clearer outside strong metropolitan and regional centres; health, irrigation, and local fiscal deficits form different, fragmented geographies. Their incomplete overlap confirms that no single income or infrastructure measure represents multidimensional capacity (Figure 2k-o).

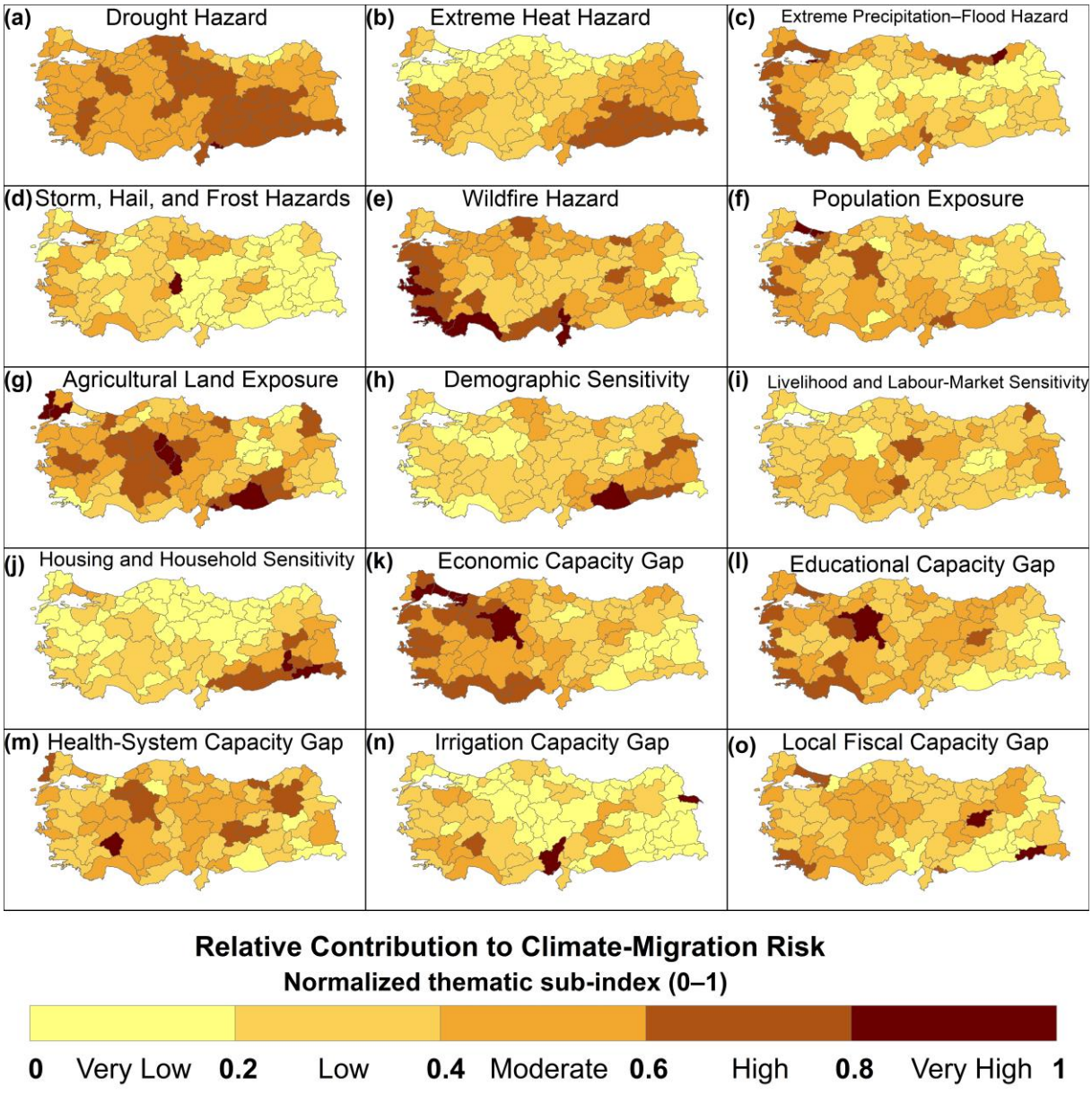


Figure 2. Province-level distribution of the 15 normalized thematic sub-indices constituting the CMRI

Together, the panels show intersecting pathways rather than one high-risk region. Hot–dry pressure, agricultural exposure, and several capacity deficits overlap in the southeast; northern and western highs arise from more selective hazards or exposures. Main components must therefore be interpreted separately.

4.2. Main components and the CMRI

Observed ranges are 0.264-0.605 for H, 0.035-0.708 for E, 0.135-0.557 for S, 0.126-0.611 for positive AC, and 0.389–0.874 for LAC. Exposure varies most because of scale differences between large cities and sparsely populated provinces. H distinguishes heat-drought, fire, and precipitation combinations despite a narrower range. S and LAC are prominent in the east and southeast; higher AC occurs mainly in the west and selected regional centres (Figure 3).

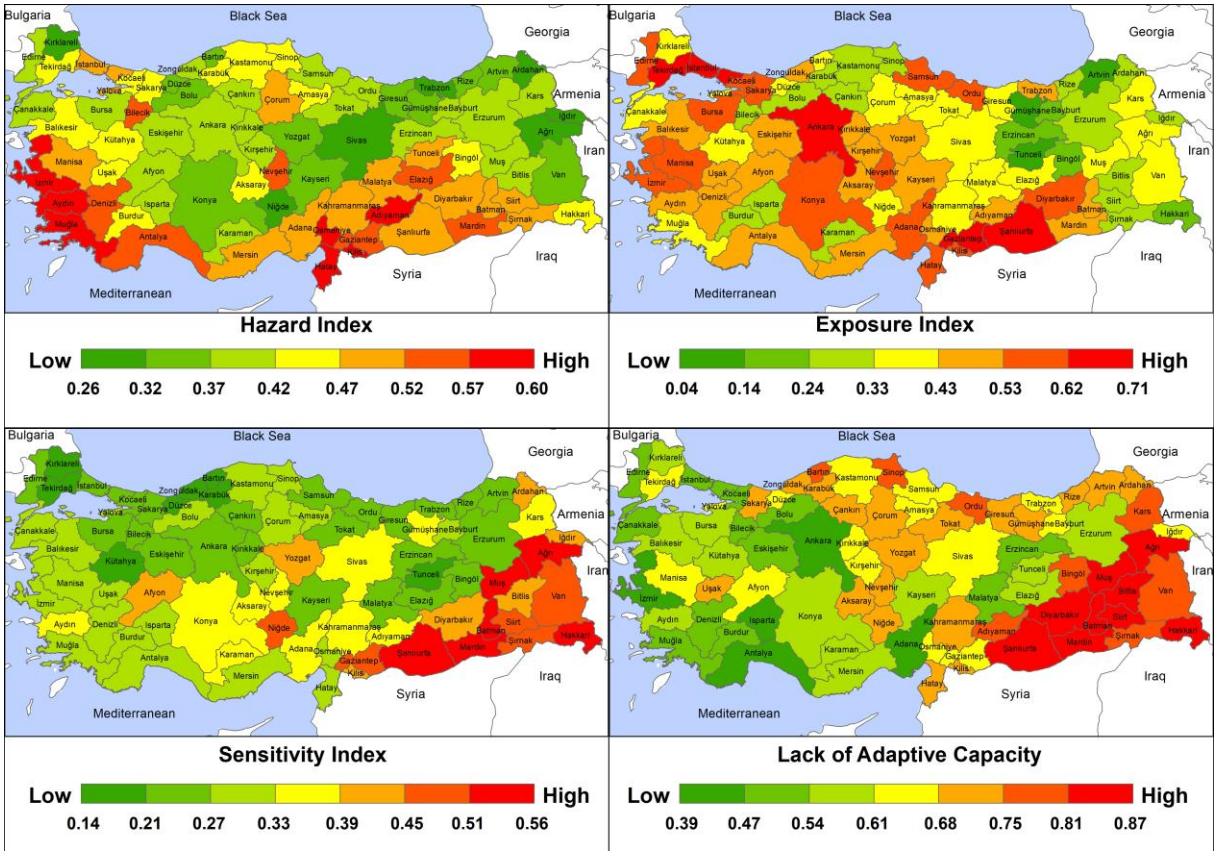


Figure 3. Normalized hazard (H), exposure (E), sensitivity (S), and lack of adaptive capacity (LAC) components by province

Note. Each panel is divided into seven equal classes within its observed range. A higher value indicates a larger relative contribution to the CMRI in every panel; colours should not be used for direct magnitude comparisons across panels.

The components form three broad profiles. In much of the southeast, high sensitivity and capacity deficits coincide with hazard and agricultural exposure. On western and southern coasts, smaller capacity deficits partly moderate high hazard. In major cities, high E is partly offset by lower S or stronger capacity. Neither one high component nor a capacity advantage determines the CMRI; component-defined directional belts are more informative than conventional regions.

The CMRI ranges from 0.303 to 0.612, with a mean of 0.432 and a median of 0.435. Using interpretive classes of fixed 0.20 width, 29 provinces are low risk, 51 are medium risk, and only Şanlıurfa is high risk; none falls in the very-low or very-high class. To show the continuous distribution more clearly, Figure 4 divides the observed range into 10 equal intervals. These visual classes are not policy thresholds. A high-score core is visible around Şanlıurfa, Mardin, Gaziantep,

Kilis, Diyarbakır, Adıyaman, Hatay, and Batman, but geographic proximity does not imply a common cause. Hot–dry hazards dominate in some provinces, while human-agricultural exposure, social sensitivity, or capacity deficits dominate in others. The high positions of Aydın and Nevşehir through different component pathways further show that the CMRI map answers "where," whereas the thematic sub-indices explain "why."

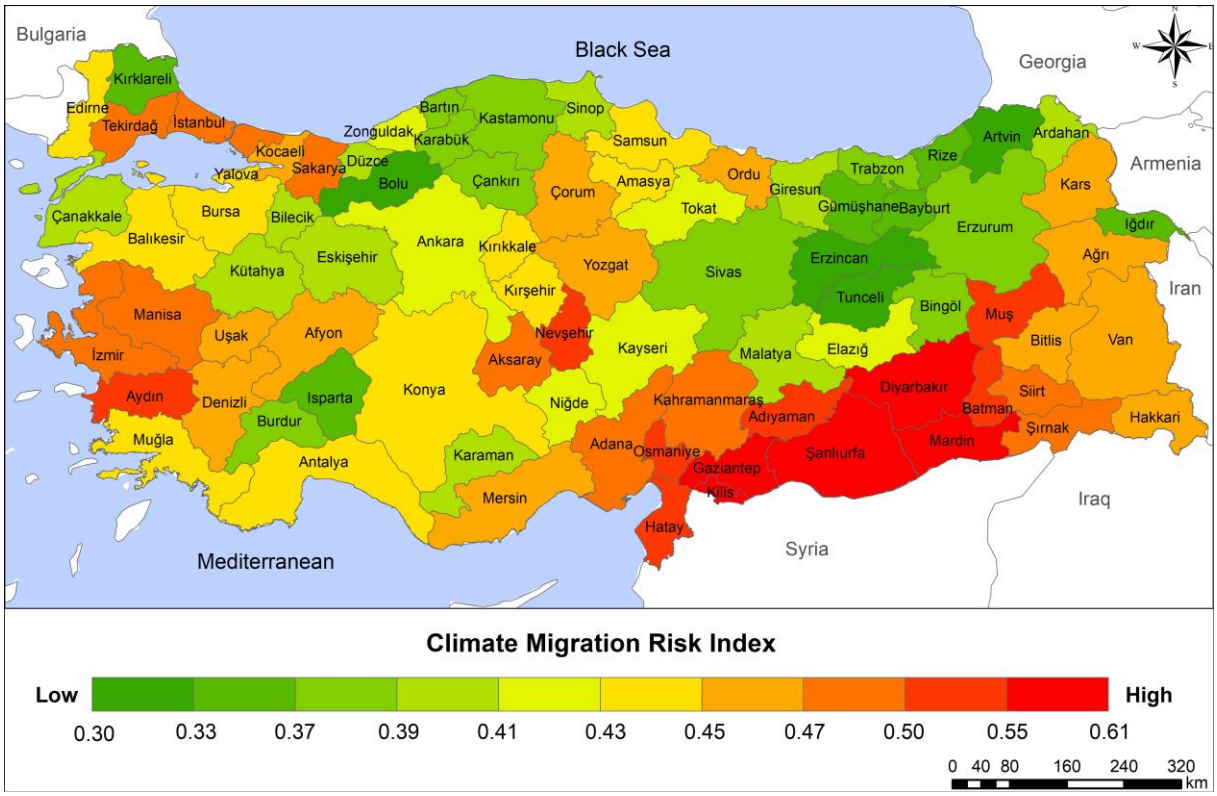


Figure 4. Province-level distribution of the Climate Migration Risk Index (CMRI) in Türkiye

Note. Continuous CMRI values are displayed in 10 equal classes across the observed range of 0.303-0.612; a higher value denotes greater relative structural climate migration risk.

The CMRI is more than a ranking map. Continuity across the eastern Mediterranean and Southeastern Anatolia reflects accumulated components, while local western and central highs show different pathways producing similar scores. Robustness analysis tests the dependence of this geography on method choices.

4.3. Model stability and comparison with migration indicators

Alternative methods preserve the main pattern. Correlations with the baseline ranking are 0.968 for equal weights, 0.957 for CRITIC, 0.983 for winsorization, and 0.975 for geometric aggregation. Mean absolute rank change is 3.14-5.14 provinces and top-20% overlap 87.5%-93.8%. Leave-one-out correlations are 0.919–0.999; removing agricultural-land share produces the largest change ($\rho = 0.919$; mean rank change = 7.11), indicating that agricultural-land exposure exerts the strongest single-indicator influence on the ranking without reversing the overall geography.

In the Monte Carlo analysis, the mean 5th-95th percentile interval is 0.029 and the median rank interval eight positions. Eleven provinces remain in the top 20% with at least 99.5% probability. The high-score core is strongly distinguished, but middle ranks are uncertain; stable cores, transition groups, and profiles are more defensible than exact ranks.

TurkStat's 2008–2025 panel shows limited, measure-dependent overlap between the CMRI and internal migration (Table 3). The weak negative association with mean 2018–2025 net migration ($\rho = -0.267$, $p = 0.016$) is not significant after controls ($\beta = -0.115$, $p = 0.291$). The full-period bivariate result ($\rho = -0.248$, $p = 0.026$) likewise disappears ($\beta = -0.140$, $p = 0.143$); both adjusted p values exceed $\alpha = 0.05$. No association appears for 2025 net migration. The inverse relationship with 2025 out-migration ($\rho = -0.432$, $p < 0.001$) persists after controls ($\beta = -0.451$, $p = 0.001$), but does not prove that risk reduces migration. Resource constraints may limit mobility, economic centres generate circulation, and net rates balance two-way flows.

Table 3. Diagnostic comparison between the CMRI and internal migration indicators

Migration indicator	n	Spearman ρ	p	Adjusted β	p
2025 net migration rate	81	0.085	0.449	0.110	0.337
Mean net migration rate, 2018–2025	81	−0.267	0.016*	−0.115	0.291
Mean net migration rate, 2008–2025	81	−0.248	0.026*	−0.140	0.143
Years of negative net migration, 2018–2025	81	0.203	0.069	0.023	0.832
2025 out-migration rate	81	−0.432	< 0.001***	−0.451	0.001**

Note. All p values are two-sided. Spearman tests use a Student's t approximation (df = 79); linear models use an HC3-robust Student's t reference distribution (residual df = 77). The decision threshold is $\alpha = 0.05$; $p \geq 0.05$ is not considered statistically significant. * $p < 0.05$. ** $p < 0.01$. *** $p < 0.001$. Adjusted coefficients are standardized. Models control for a binary 2023 earthquake-affected-province indicator and the 2025 foreign-population share. Because foreign nationals entered the TurkStat series in 2018, 2018–2025 is the primary period and 2008–2025 is a sensitivity comparison. Results do not imply causality.

Table 3 shows that weak period-average associations disappear after controls and that single-year indicators do not provide consistent validation. This clarifies rather than weakens the construct: the CMRI compares settings in which migration pressure may arise; it does not predict realized flows.

5. Discussion

Climate migration risk in Türkiye is not a direct extension of hazard intensity. High CMRI values arise where climate pressure coincides with human or agricultural exposure, social sensitivity, and limited capacity. This shows how environmental change operates through livelihoods, institutions, and inequality rather than as an autonomous migration cause. The CMRI distinguishes risk combinations that may become mobility pressure; it does not predict migrant numbers.

This multidimensional structure helps explain divergent climate–migration coefficients. Temperature effects vary with income, and temperature and rainfall shocks produce selective mobility in agricultural economies (Beine & Parsons, 2015; Mastrorillo et al., 2016; Mueller et al., 2014). Conflict

and asylum studies also show political and economic mediation of climate signals (Abel et al., 2019; Missirian & Schlenker, 2017). Turkish provincial profiles differ empirically but support the common mechanism: physical pressure matters through exposure, livelihood sensitivity, and capacity.

The concentration of risk in southern and southeastern provinces is broadly consistent with literature on drought, land degradation, and agricultural vulnerability in Türkiye (Çelik et al., 2026; Serkendiz et al., 2023; Türkeş, 2017; Türkeş et al., 2020; Yurtseven & Türkeş, 2026). The observed expansion of semi-arid and Mediterranean climates and projected shifts toward warmer, drier climate types suggest that this spatial overlap may persist (Türkeş & Yurtseven, 2025). Field evidence from different Turkish regions identifies the cumulative effects of drought on agricultural production and rural livelihoods as a major mechanism increasing migration potential (Tekin & Deniz, 2025). The results nevertheless show that drought alone cannot explain this belt. Some provinces within the upper-score group stand out through H, others through E and S, and others through capacity deficits. Partial similarity—but not identical rankings—relative to general disaster-vulnerability maps is therefore expected: the CMRI, which combines social vulnerability with specific hazard and mobility pathways, does not measure the same construct (Yükseler & Tenikler, 2025).

Contrasting profiles show the method's value. Strong capacity and low sensitivity can partly offset high population exposure, while weak capacity can turn moderate hazard into high risk. This matches evidence that vulnerability rankings depend on indicators, scale, and hierarchy (Hinojos et al., 2026). Removing agricultural-land share causes the largest leave-one-out rank change, confirming the livelihood pathway. Agricultural land is not intrinsically risky: assigning land to E, registered farm employment to S, and irrigation to AC separates three sectoral functions and shows why the final score requires its components (Hinkel, 2011).

Turkish mobility patterns support this interpretation. Climate and labour risks across the residence, workplace, and temporary accommodation of seasonal farmworkers reveal vulnerabilities hidden by provincial means (Kavak et al., 2026). Policies do not reduce vulnerability when they leave labour relations and unequal resource access unchanged (Turhan et al., 2015). Conversely, movement toward higher settlements in Antalya shows climate pressure becoming local adaptation when resources and housing are accessible (Ustaoğlu et al., 2026). National net migration omits temporary, circular, and within-province movement, limiting its expected overlap with the CMRI.

The comparison clarifies the boundary between structural risk and realized mobility. Mean 2018–2025 net migration loses its weak association after controls, and the single-year net rate is unrelated. The inverse out-migration association does not mean that risk reduces departures. Net migration reflects economic attraction, education, housing, life course, and networks; climate stress can raise migration aspirations while income loss reduces mobility capacity. Low recorded departure can therefore coexist with high risk (de Haas, 2021; Garip & Reed, 2025). Migration may be adaptive when resourced,

create vulnerability when unplanned, or yield to involuntary immobility (Adams, 2016; McLeman & Smit, 2006; Zickgraf, 2021).

The high-score core does not depend on any single weight, outlier, or aggregation rule, but movement in the middle ranks reveals greater uncertainty. Weights encode theoretical judgments, linear aggregation permits partial compensation, and min–max values depend on the provincial distribution. High correlations show stability under plausible alternatives, not assumption-free truth. Uncertainty intervals and risk profiles are preferable to a definitive league table.

Limitations are integral to this interpretation. Provincial means conceal neighbourhood, class, gender, and urban–rural differences. Administrative boundaries are not the natural boundaries of climate systems or migration networks. Periods are not fully synchronous, and some capacity indicators do not measure who can actually access resources. Record-based event densities may also reflect reporting differences. Longitudinal household data at finer spatial scales, together with measures of migration intentions, movement costs, temporary mobility, and involuntary immobility, should test the mechanisms through which the profiles identified here translate into migration or staying. Maps should not portray people as homogeneous populations destined to move (Bettini, 2013).

Policy requires adaptation packages differentiated by the dominant pathway. Hot–dry and agricultural profiles need integrated water management, livelihood diversification, and social protection, consistent with assessments linking climate, farming, food security, rural life, and production planning in Türkiye (Türkeş, 2026). Coastal areas need heat, fire, and flood preparedness; metropolitan areas need housing and service continuity under dense exposure. The CMRI does not prescribe policy, but identifies where each component warrants investigation, linking national screening to place-based research.

6. Conclusion

Combining 25 indicators under H, E, S, and AC shows that high climate migration risk across Türkiye's 81 provinces arises from intersections of physical pressure, human and agricultural exposure, sensitivity, and capacity deficits-not one hazard. Similar CMRI values follow different pathways, limiting prioritization by one climate measure or a development ranking. Stability across alternative methods supports the identification of a high-score core, while the limited and measure-dependent overlap with migration data supports the interpretation that the index captures structural risk rather than realized migration flows.

The CMRI ranges from 0.303 to 0.612, forming a high-score core in Southeastern Anatolia and the eastern Mediterranean, although dominant pathways vary by province. Correlations of 0.957-0.983 with alternative weighting and aggregation models, leave-one-out values of at least 0.919, and 11 provinces remaining in the top 20% in at least 99.5% of Monte Carlo draws demonstrate stability. Wider middle-rank uncertainty favours stable cores and component profiles over exact positions.

The CMRI is neither a stand-alone decision rule nor a forecast. Scores require each province's hazard, sensitivity, and capacity profile. Water and livelihood security, health, social protection, housing, and local services should follow that profile. Regular updates and tests with sub-provincial household mobility data are the next step toward equitable policies supporting both safe staying and voluntary, safe mobility.

References

Abel, G. J., Brottrager, M., Crespo Cuaresma, J., & Muttarak, R. (2019). Climate, conflict and forced migration. *Global Environmental Change, 54*, 239-249. https://doi.org/10.1016/j.gloenvcha.2018.12.003

Adams, H. (2016). Why populations persist: Mobility, place attachment and climate change. *Population and Environment, 37*(4), 429-448. https://doi.org/10.1007/s11111-015-0246-3

Bağçacı, S. Ç., Yücel, İ., Düzenli, E., & Yılmaz, M. T. (2021). Intercomparison of the expected change in the temperature and the precipitation retrieved from CMIP6 and CMIP5 climate projections: A Mediterranean hot spot case, Turkey. *Atmospheric Research, 256*, 105576. https://doi.org/10.1016/j.atmosres.2021.105576

Baldwin, A. (2013). Racialisation and the figure of the climate-change migrant. *Environment and Planning A, 45*(6), 1474-1490. https://doi.org/10.1068/a45388

Beine, M., & Parsons, C. (2015). Climatic factors as determinants of international migration. *The Scandinavian Journal of Economics, 117*(2), 723-767. https://doi.org/10.1111/sjoe.12098

Bettini, G. (2013). Climate barbarians at the gate? A critique of apocalyptic narratives on 'climate refugees'. *Geoforum, 45*, 63-72. https://doi.org/10.1016/j.geoforum.2012.09.009

Black, R., Adger, W. N., Arnell, N. W., Dercon, S., Geddes, A., & Thomas, D. (2011a). The effect of environmental change on human migration. *Global Environmental Change, 21*(Suppl. 1), S3-S11. https://doi.org/10.1016/j.gloenvcha.2011.10.001

Black, R., Bennett, S. R. G., Thomas, S. M., & Beddington, J. R. (2011b). Migration as adaptation. *Nature, 478*(7370), 447-449. https://doi.org/10.1038/478477a

Boas, I., Farbotko, C., Adams, H., Sterly, H., Bush, S., van der Geest, K., Wiegel, H., Ashraf, H., Baldwin, A., Bettini, G., Blondin, S., de Bruijn, M., Durand-Delacre, D., Fröhlich, C., Gioli, G., Guaita, L., Hut, E., Jarawura, F. X., Lamers, M., . . . Hulme, M. (2019). Climate migration myths. *Nature Climate Change, 9*(12), 901-903. https://doi.org/10.1038/s41558-019-0633-3

Borderon, M., Sakdapolrak, P., Muttarak, R., Kebede, E., Pagogna, R., & Sporer, E. (2019). Migration influenced by environmental change in Africa: A systematic review of empirical evidence. *Demographic Research, 41*, 491-544. https://doi.org/10.4054/DemRes.2019.41.18

Cattaneo, C., Beine, M., Fröhlich, C. J., Kniveton, D., Martínez-Zarzoso, I., Mastrorillo, M., Millock, K., Piguet, E., & Schraven, B. (2019). Human migration in the era of climate change. *Review of Environmental Economics and Policy, 13*(2), 189-206. https://doi.org/10.1093/reep/rez008

Cattaneo, C., & Peri, G. (2016). The migration response to increasing temperatures. *Journal of Development Economics, 122*, 127-146. https://doi.org/10.1016/j.jdeveco.2016.05.004

Çelik, M. A., Duran, V., & Türkeş, M. (2026). Modeling drought dynamics in Türkiye: A novel SIR-based differential equation framework. *Acta Geophysica, 74*, Article 262. https://doi.org/10.1007/s11600-026-01977-3

Copernicus Land Monitoring Service. (2018). *CORINE Land Cover 2018 (vector), Europe, 6-yearly* [Data set]. European Environment Agency. https://doi.org/10.2909/71c95a07-e296-44fc-b22b-415f42acfdf0

Cutter, S. L., Boruff, B. J., & Shirley, W. L. (2003). Social vulnerability to environmental hazards. *Social Science Quarterly, 84*(2), 242-261. https://doi.org/10.1111/1540-6237.8402002

Cutter, S. L., & Finch, C. (2008). Temporal and spatial changes in social vulnerability to natural hazards. *Proceedings of the National Academy of Sciences, 105*(7), 2301-2306. https://doi.org/10.1073/pnas.0710375105

de Haas, H. (2021). A theory of migration: The aspirations-capabilities framework. *Comparative Migration Studies, 9*, 8. https://doi.org/10.1186/s40878-020-00210-4

Devlet Su İşleri Genel Müdürlüğü. (2025). *DSİ 2024 yılı resmî su kaynakları istatistikleri* [Data set]. https://www.dsi.gov.tr/Sayfa/Detay/2186

Diakoulaki, D., Mavrotas, G., & Papayannakis, L. (1995). Determining objective weights in multiple criteria problems: The CRITIC method. *Computers & Operations Research, 22*(7), 763-770. https://doi.org/10.1016/0305-0548(94)00059-H

Erlat, E., Türkeş, M., & Aydın-Kandemir, F. (2021). Observed changes and trends in heatwave characteristics in Turkey since 1950. *Theoretical and Applied Climatology, 145*, 137-157. https://doi.org/10.1007/s00704-021-03620-1

494 European Commission, Eurostat. (2024). *GISCO: Geographical information and maps* [Data set]. Retrieved August 27,
495 2026, from https://ec.europa.eu/eurostat/web/gisco/geodata/statistical-units/territorial-units-statistics

496 Füssel, H.-M. (2007). Vulnerability: A generally applicable conceptual framework for climate change research. *Global*
497 *Environmental Change, 17*(2), 155-167. https://doi.org/10.1016/j.gloenvcha.2006.05.002

498 Garip, F., & Reed, C. A. (2025). Climate change and human mobility: Considering context, mechanisms, and selectivity.
499 *Population and Development Review, 51*(1), 449-489. https://doi.org/10.1111/padr.12716

500 Greco, S., Ishizaka, A., Tasiou, M., & Torrisi, G. (2019). On the methodological framework of composite indices: A review
501 of issues of weighting, aggregation, and robustness. *Social Indicators Research, 141*, 61-94.
502 https://doi.org/10.1007/s11205-017-1832-9

503 Hazine ve Maliye Bakanlığı. (2026). *İller itibarıyla mahallî yönetim bütçe istatistikleri, 2006-2026* [Data set]. Retrieved
504 August 27, 2026, from https://muhasebat.hmb.gov.tr/iller-itibariyle-mahalli-yonetim-butce-istatistikleri-2006-2026

505 Hersbach, H., Bell, B., Berrisford, P., Hirahara, S., Horányi, A., Muñoz-Sabater, J., Nicolas, J., Peubey, C., Radu, R.,
506 Schepers, D., Simmons, A., Soci, C., Abdalla, S., Abellan, X., Balsamo, G., Bechtold, P., Biavati, G., Bidlot, J.,
507 Bonavita, M., . . . Thépaut, J.-N. (2020). The ERA5 global reanalysis. *Quarterly Journal of the Royal Meteorological*
508 *Society, 146*(730), 1999-2049. https://doi.org/10.1002/qj.3803

509 Hinkel, J. (2011). Indicators of vulnerability and adaptive capacity: Towards a clarification of the science-policy interface.
510 *Global Environmental Change, 21*(1), 198-208. https://doi.org/10.1016/j.gloenvcha.2010.08.002

511 Hinojos, S., Roscoe, K., & Grady, C. (2026). Examining the role of indicators and scale in social vulnerability index
512 construction: A comparative geospatial analysis of inductive and hierarchical models. *Applied Geography, 186*,
513 103822. https://doi.org/10.1016/j.apgeog.2025.103822

514 Hoffmann, R., Dimitrova, A., Muttarak, R., Crespo Cuaresma, J., & Peisker, J. (2020). A meta-analysis of country-level
515 studies on environmental change and migration. *Nature Climate Change, 10*(10), 904-912.
516 https://doi.org/10.1038/s41558-020-0898-6

517 Hoffmann, R., Šedová, B., & Vinke, K. (2021). Improving the evidence base: A methodological review of the quantitative
518 climate migration literature. *Global Environmental Change, 71*, 102367.
519 https://doi.org/10.1016/j.gloenvcha.2021.102367

520 Hunter, L. M., Luna, J. K., & Norton, R. M. (2015). Environmental dimensions of migration. *Annual Review of Sociology,*
521 *41*, 377-397. https://doi.org/10.1146/annurev-soc-073014-112223

522 Intergovernmental Panel on Climate Change. (2022). *Climate change 2022: Impacts, adaptation and vulnerability: Working*
523 *Group II contribution to the Sixth Assessment Report of the Intergovernmental Panel on Climate Change* (H.-O.
524 Pörtner, D. C. Roberts, M. Tignor, E. S. Poloczanska, K. Mintenbeck, A. Alegría, M. Craig, S. Langsdorf, S. Löschke,
525 V. Möller, A. Okem, & B. Rama, Eds.). Cambridge University Press. https://doi.org/10.1017/9781009325844

526 Kavak, S., Işlar, M., & Olsson, L. (2026). Agri-labour mobility in a changing climate: A systems approach to vulnerability
527 and precarity among migrant farmworkers. *World Development, 202*, 107329.
528 https://doi.org/10.1016/j.worlddev.2026.107329

529 MacKinnon, J. G., & White, H. (1985). Some heteroskedasticity-consistent covariance matrix estimators with improved finite
530 sample properties. *Journal of Econometrics, 29*(3), 305-325. https://doi.org/10.1016/0304-4076(85)90158-7

531 Malczewski, J. (2000). On the use of weighted linear combination method in GIS: Common and best practice approaches.
532 *Transactions in GIS, 4*(1), 5-22. https://doi.org/10.1111/1467-9671.00035

533 Malczewski, J. (2006). GIS-based multicriteria decision analysis: A survey of the literature. *International Journal of*
534 *Geographical Information Science, 20*(7), 703-726. https://doi.org/10.1080/13658810600661508

535 Mastrorillo, M., Licker, R., Bohra-Mishra, P., Fagiolo, G., Estes, L. D., & Oppenheimer, M. (2016). The influence of climate
536 variability on internal migration flows in South Africa. *Global Environmental Change, 39*, 155-169.
537 https://doi.org/10.1016/j.gloenvcha.2016.04.014

538 McLeman, R., & Smit, B. (2006). Migration as an adaptation to climate change. *Climatic Change, 76*(1-2), 31-53.
539 https://doi.org/10.1007/s10584-005-9000-7

540 Meteoroloji Genel Müdürlüğü. (2023). *Fevkalade meteorolojik olay kayıtları (FEVK), 2008-2022* [Data set]. Retrieved
541 August 27, 2026, from https://www.mgm.gov.tr/

542 Mijani, N., Shahpari Sani, D., Dastaran, M., Karimi Firozjaei, H., Argany, M., & Mahmoudian, H. (2022). Spatial modeling
543 of migration using GIS-based multi-criteria decision analysis: A case study of Iran. *Transactions in GIS, 26*(2), 645-
544 668. https://doi.org/10.1111/tgis.12873

545 Missirian, A., & Schlenker, W. (2017). Asylum applications respond to temperature fluctuations. *Science, 358*(6370), 1610-
546 1614. https://doi.org/10.1126/science.aao0432

547 Mueller, V., Gray, C., & Kosec, K. (2014). Heat stress increases long-term human migration in rural Pakistan. *Nature*
548 *Climate Change, 4*(3), 182-185. https://doi.org/10.1038/nclimate2103

549 Organisation for Economic Co-operation and Development, & European Commission, Joint Research Centre. (2008).
550 *Handbook on constructing composite indicators: Methodology and user guide*. OECD Publishing.
551 https://doi.org/10.1787/9789264043466-en

Orman Genel Müdürlüğü. (2022). *Ormancılık istatistikleri* [Data set]. Retrieved August 27, 2026, from https://www.ogm.gov.tr/tr/e-kutuphane/resmi-istatistikler

Paul, B. K., Rahman, M. K., Crawford, T., Curtis, S., Miah, M. G., Islam, M. R., & Islam, M. S. (2020). Explaining mobility using the community capital framework and place attachment concepts: A case study of riverbank erosion in the Lower Meghna Estuary, Bangladesh. *Applied Geography, 125*, 102199. https://doi.org/10.1016/j.apgeog.2020.102199

Piguet, E. (2010). Linking climate change, environmental degradation, and migration: A methodological overview. *WIREs Climate Change, 1*(4), 517-524. https://doi.org/10.1002/wcc.54

Preston, B. L., Yuen, E. J., & Westaway, R. M. (2011). Putting vulnerability to climate change on the map: A review of approaches, benefits, and risks. *Sustainability Science, 6*(2), 177-202. https://doi.org/10.1007/s11625-011-0129-1

Republic of Türkiye Ministry of Environment, Urbanisation and Climate Change. (2023). *Eighth national communication and fifth biennial report of Türkiye under the UNFCCC*. https://unfccc.int/sites/default/files/resource/8NC-5BR%20T%C3%BCrkiye.pdf

Rufat, S., Tate, E., Burton, C. G., & Maroof, A. S. (2015). Social vulnerability to floods: Review of case studies and implications for measurement. *International Journal of Disaster Risk Reduction, 14*, 470-486. https://doi.org/10.1016/j.ijdrr.2015.09.013

Saisana, M., Saltelli, A., & Tarantola, S. (2005). Uncertainty and sensitivity analysis techniques as tools for the quality assessment of composite indicators. *Journal of the Royal Statistical Society: Series A (Statistics in Society), 168*(2), 307-323. https://doi.org/10.1111/j.1467-985X.2005.00350.x

Sakdapolrak, P., Borderon, M., & Sterly, H. (2024). The limits of migration as adaptation: A conceptual approach towards the role of immobility, disconnectedness and simultaneous exposure in translocal livelihood systems. *Climate and Development, 16*(2), 87-96. https://doi.org/10.1080/17565529.2023.2180318

Schewel, K., Dickerson, S., Madson, B., & Nagle Alverio, G. (2024). How well can we predict climate migration? A review of forecasting models. *Frontiers in Climate, 5*, 1189125. https://doi.org/10.3389/fclim.2023.1189125

Schürmann, A., Kleemann, J., Teucher, M., & Conrad, C. (2024). Mapping socio-environmental vulnerability to assess rural migration in Ghana. *Applied Geography, 167*, 103283. https://doi.org/10.1016/j.apgeog.2024.103283

Serkendiz, H., Tatli, H., Özcan, H., Çetin, M., & Sungur, A. (2023). Multidimensional assessment of agricultural drought vulnerability based on socioeconomic and biophysical indicators. *International Journal of Disaster Risk Reduction, 98*, 104121. https://doi.org/10.1016/j.ijdrr.2023.104121

Sosyal Güvenlik Kurumu. (2025). *2024 yılı istatistik yıllığı* [Data set]. https://www.sgk.gov.tr/istatistik/yillik/fcd5e59b-6af9-4d90-a451-ee7500eb1cb4/

Tate, E. (2012). Social vulnerability indices: A comparative assessment using uncertainty and sensitivity analysis. *Natural Hazards, 63*(2), 325-347. https://doi.org/10.1007/s11069-012-0152-2

Tate, E. (2013). Uncertainty analysis for a social vulnerability index. *Annals of the Association of American Geographers, 103*(3), 526-543. https://doi.org/10.1080/00045608.2012.700616

T.C. Sağlık Bakanlığı. (2024). *Sağlık istatistikleri yıllığı 2023*. https://www.saglik.gov.tr/TR-107086/saglik-istatistikleri-yilligi-2023.html

T.C. Sağlık Bakanlığı. (2025). *Sağlık istatistikleri yıllığı 2024*. https://www.saglik.gov.tr/TR-114952/saglik-istatistikleri-yilligi-2024.html

Tekin, M. K., & Deniz, O. (2025). İklim değişikliği kaynaklı göç potansiyeli: Türkiye üzerine çok boyutlu bir alan araştırması. Coğrafi Bilimler Dergisi, 23(1), 236–263. https://doi.org/10.33688/aucbd.1517859

Thomas, A., Sircar, A., Abu, M., Boyd, E., Howe, L., Pinho, P., Scown, M., & Shenga, C. (2025). Immobility in the context of climate change. *Annual Review of Environment and Resources, 50*, 47-66. https://doi.org/10.1146/annurev-environ-121923-120443

Turhan, E., Zografos, C., & Kallis, G. (2015). Adaptation as biopolitics: Why state policies in Turkey do not reduce the vulnerability of seasonal agricultural workers to climate change. Global Environmental Change, 31, 296–306. https://doi.org/10.1016/j.gloenvcha.2015.02.003

Türkeş, M. (2017). Türkiye'nin iklimsel değişkenlik ve sosyo-ekolojik göstergeler açısından kuraklıktan etkilenebilirlik ve risk çözümlemesi. *Ege Coğrafya Dergisi, 26*(2), 47-70.

Türkeş, M. (2026). Küresel gelişmelerin, iklim krizinin ve uluslararası ticaret politikalarının tarımsal üretim, gıda güvenliği, kırsal yaşam ve üretim planlaması üzerindeki etkileri: Küresel ve Türkiye bağlamında bilimsel bir değerlendirme. *İktisat ve Toplum, 189*, 23–32.

Türkeş, M., Öztaş, T., Tercan, E., Erpul, G., Karagöz, A., Dengiz, O., Doğan, O., Şahin, K., & Avcıoğlu, B. (2020). Desertification vulnerability and risk assessment for Turkey via an analytical hierarchy process model. *Land Degradation & Development, 31*(2), 205-214. https://doi.org/10.1002/ldr.3441

Türkeş, M., & Tatlı, H. (2009). Use of the standardized precipitation index (SPI) and a modified SPI for shaping the drought probabilities over Turkey. *International Journal of Climatology, 29*(15), 2270-2282. https://doi.org/10.1002/joc.1862

Türkeş, M., Tekin, M. K., & Salli, D. (2026). Theoretical and conceptual evaluation of climate-related displacement and mobility. *The Anthropocene Review*. Advance online publication. https://doi.org/10.1177/20530196261434015

Türkeş, M., & Yurtseven, N. (2025). Observed and projected geographical and temporal changes in the Köppen-Geiger climate types in Türkiye. *Theoretical and Applied Climatology, 156*, Article 154. https://doi.org/10.1007/s00704-024-05346-2

Türkiye İstatistik Kurumu. (2026). *TÜİK Veri Portalı* [Database]. Retrieved August 27, 2026, from https://veriportali.tuik.gov.tr/

Ustaoğlu, B., Sunata, U., Kaçmaz, M., & Birkök, M. C. (2026). Climate change influenced migration: Vertical residential mobility as an adaptation strategy in Antalya, Türkiye. *Climate Services, 44*, 100713. https://doi.org/10.1016/j.cliser.2026.100713

Vicente-Serrano, S. M., Beguería, S., & López-Moreno, J. I. (2010). A multiscalar drought index sensitive to global warming: The standardized precipitation evapotranspiration index. *Journal of Climate, 23*(7), 1696-1718. https://doi.org/10.1175/2009JCLI2909.1

World Bank. (2021, September 13). *Climate change could force 216 million people to migrate within their own countries by 2050* [Press release]. https://www.worldbank.org/en/news/press-release/2021/09/13/climate-change-could-force-216-million-people-to-migrate-within-their-own-countries-by-2050

World Bank. (2026). *Climate Change Knowledge Portal* [Database]. Retrieved August 27, 2026, from https://climateknowledgeportal.worldbank.org/

Yıldız, M. B., Nacar, S., Şan, M., & Kankal, M. (2025). Spatial and temporal patterns of drought under different scenarios for Türkiye in the 21st century. *Physics and Chemistry of the Earth, Parts A/B/C, 140*, 104028. https://doi.org/10.1016/j.pce.2025.104028

Yükseler, M., & Tenikler, G. (2025). Multidimensional assessment of social vulnerability to natural hazards in Türkiye using different methods. *Sustainable Cities and Society, 131*, 106749. https://doi.org/10.1016/j.scs.2025.106749

Yurtseven, N., & Türkeş, M. (2026). A comprehensive assessment of drought dynamics in Türkiye: An integrated spatiotemporal analysis of trends, variability and persistence. *International Journal of Climatology*, e70541. https://doi.org/10.1002/joc.70541

Zickgraf, C. (2021). Theorizing (im)mobility in the face of environmental change. *Regional Environmental Change, 21*, 126. https://doi.org/10.1007/s10113-021-01839-2

Ethics approval and consent to participate

Not applicable.

Consent for publication

Not applicable.

Competing Interests

The authors have no relevant financial or non-financial interests to disclose.

Author contributions

Mehmet Kadri Tekin: Conceptualization, Methodology, Software, Formal analysis, Investigation, Data Curation, Writing - Original Draft, Writing - Review & Editing, Visualization.

Murat Türkeş: Conceptualization, Methodology, Supervision, Validation, Writing - Review & Editing.

Funding

The authors declare that no funds, grants, or other support were received during the preparation of this manuscript.

Availability of data and materials

The datasets generated during and/or analyzed during the current study are available from the corresponding author on reasonable request.